Available online at www.sciencedirect.com
ScienceDirect
Journal of Power Sources 164 (2007) 555–560
JOURNAL OF POWER SOURCES
www.elsevier.com/locate/jpowsour

Short communication

Structural designing of Pt-CeO_2/CNTs for methanol electro-oxidation

Jianshe Wang [a,b], Jingyu Xi [b], Yuxia Bai [a], Yi Shen [a], Jie Sun [c], Liquan Chen [a,b], Wentao Zhu [a], Xinping Qiu [a,b,*]

[a] *Key Laboratory of Organic Optoelectronics and Molecular Engineering, Department of Chemistry, Tsinghua University, Beijing 100084, China*
[b] *Laboratory of Advanced Power Sources, Graduate School at Shenzhen, Tsinghua University, Shenzhen 518055, China*
[c] *Institute of Chemical Defense, Beijing 102205, China*

Received 28 August 2006; received in revised form 5 November 2006; accepted 17 November 2006

Abstract

In an attempt to utilize CeO_2 as a co-catalyst with Pt for methanol electro-oxidation, Pt-CeO_2/CNTs were prepared through structural designing by adsorbing Pt nanoparticles on CeO_2 coated CNTs. X-ray Diffraction (XRD), energy dispersive X-ray spectroscopy (EDX) were used to analyze the composition of the prepared catalysts. Zeta potential analysis, high resolution transmission electron microscopy (HRTEM) and cyclic voltammetry (CV) methods indicated that Pt nanoparticles are selectively adsorbed on CNTs other than CeO_2 surface. Pt-CeO_2/CNTs were compared with Pt supported on CNTs in terms of electrochemical active surface (EAS) areas, methanol electro-oxidation activity, and chronoamperometry, results indicating that CeO_2 can enhance the catalytic activity of Pt for methanol electro-oxidation with no apparent decrease of EAS. The CO stripping test showed that CeO_2 can make CO stripped at a lower potential, which is helpful for CO and methanol electro-oxidation.

Keywords: Direct methanol fuel cell (DMFC); Methanol electro-oxidation; Pt-CeO_2/CNTs

1. Introduction

Although direct methanol fuel cell (DMFC) is proposed to be a kind of promising power source due to its high energy conversion efficiency, some obstacles, such as the low methanol electro-oxidation kinetics and methanol permeation across the proton exchange membrane, still exist for its commercialization. It is generally accepted that the CO species produced during the electro-oxidation of methanol is the main reason for the low kinetics of methanol electro-oxidation [1]. To deal with the CO poisoning issue, the most widely accepted strategy is to use Pt-based alloys or Pt/metal oxide composites based upon the bi-functional mechanism [2] and the electronic effect [3]. Recently, more and more works have been focused on other systems, such as Pt–Sn [4,5], Pt–Ni [6], Pt–Mo [7], and Pt–WO_3 [8], though many researches on Pt/Ru and Pt/RuO_xH_y, the benchmark anode catalysts for DMFC, have been done.

CeO_2, one of the most widely used rare earth metal oxide catalysts, is efficient for gaseous CO oxidation [9]. It is economic to replace ruthenium if cerium oxide can match ruthenium in catalytic activity due to the low cost of cerium. Till now, although CeO_2 has been shown to be effective in alkaline fuel cells [10], there are few reports concerning the application of cerium oxide in DMFC maybe due to its low electron conductivity [11]. For good methanol electro-oxidation catalyst, electron conductivity and CO tolerance are two important aspects. Compared with Ru, CeO_2 has no good electron conductivity, although it can promote CO oxidation significantly. Therefore, to explore the possibility of using CeO_2 as co-catalyst in methanol electro-oxidation, it deserves study how to design good catalyst structure with less side-effect resulting from the bad electron conductivity of CeO_2.

In this research we prepared Pt catalyst supported on CeO_2/carbon nanotubes (CNTs) composite (denoted as Pt-CeO_2/CNTs) with designed structure and characterized the catalyst by transmission electron microscopy (TEM), high resolution TEM (HRTEM), X-ray diffraction (XRD), energy dispersive X-ray spectroscopy (EDX), zeta potential analyzer, cyclic voltammetry (CV), chronoamperometry, and CO stripping. The results show that the Pt catalyzing activity is improved

* Corresponding author at: Key Laboratory of Organic Optoelectronics and Molecular Engineering, Department of Chemistry, Tsinghua University, Beijing 100084, China. Tel.: +86 10 62794235; fax: +86 10 62794234.
E-mail address: qiuxp@mail.tsinghua.edu.cn (X. Qiu).

0378-7753/$ – see front matter © 2006 Elsevier B.V. All rights reserved.
doi:10.1016/j.jpowsour.2006.11.041

while there is nearly no disadvantage from the bad electron conductivity of CeO_2.

2. Experimental

Multi-walled carbon nanotubes (MWCNTs) were obtained from Chemical Engineering Department, Tsinghua University. The MWCNTs were treated by boiling the as-received MWCNTs in HNO_3 for 3 h, rinsed with copious water, dried and ground. The thus oxidized MWCNTs were denoted as O-CNTs. Poly(diallyldimethylammonium chloride) (PDDA, 35 wt.% in water, $M_w < 100{,}000\ g\ mol^{-1}$) were obtained from Aldrich and used as received. The PDDA coated MWCNTs were prepared as follows: O-CNTs were firstly dispersed in PDDA solutions ($0.1\ mg\ mL^{-1}$) for 1 h with sonification and then centrifuged and rinsed five times with deionized water, dried in oven under 100 °C and finally ground for later use. The PDDA coated O-CNTs were denoted as PO-CNTs. CeO_2 was deposited onto the PO-CNTs by drop-wise adding $NH_3{\cdot}H_2O$ into a beaker containing PO-CNTs and $Ce(NO_3)_3$ aqueous solution under magnetic stirring. After rinsing with water, the composite product was dried under 100 °C and ground before following use. The CeO_2 deposited PO-CNTs were denoted as CPO-CNTs.

Pt particles were prepared by microwave heating of ethylene glycol (EG) solutions of Pt precursor salts [12]. In a typical process, certain amount of $H_2PtCl_6{\cdot}6H_2O$ was dissolved in 50 mL NaOH EG solution in a 100 mL beaker, in which the concentration of NaOH is 0.07 M. The beaker was placed in the center of a household microwave oven (*Glanz* brand microwave, 750 W) and heated for 60 s.

The above prepared CPO-CNTs was dispersed in water under magnetic agitation and then certain amount of the EG suspension of the prepared Pt particles was added drop-wise to the aqueous suspension. After 2 h adsorption of Pt particles on CPO-CNTs, the suspension was filtered, washed with deionized water and dried under 105 °C. The prepared catalyst was denoted as Pt-CPO-CNTs. In the prepared Pt-CPO-CNTs catalyst the theoretical content of CeO_2 and Pt were 30% and 20%, respectively. For comparison, the Pt nanoparticles were also adsorbed on the O-CNTs and the obtained catalysts were denoted as Pt-O-CNTs.

The morphology of Pt-O-CNTs, CPO-CNTs, and Pt-CPO-CNTs were investigated using transmission electron microscopy (TEM, JEOL model JEM-1200EX) and high resolution transmission electron microscopy (HRTEM). The zeta potentials of the samples were measured using zeta potential analyzer (Brookhaven Instruments Co., USA). The XRD patterns were recorded on a Rigaku X-ray diffractometer using Cu Kα as radiation source. The EDX analysis was performed at 150 kV using an energy dispersive X-ray spectrometer (OXFORD INCA 300) attached to the microscope.

Electrochemical reactivity of the catalysts was measured by cyclic voltammetry (CV) using a three-electrode cell at the Solartron electrochemical workstation (Solartron 1287BZ). The working electrode was a gold plate covered with a thin layer of Nafion-impregnated catalyst. As a typical process, about 1 mg catalyst sample was ultrasonically mixed with Nafion EG solution to form homogeneous ink which was cast on the gold plate. Pt gauze and a saturated calomel electrode (SCE) were used as counter electrode and reference electrode, respectively. All potentials in this report are quoted versus SCE. CV test was conducted at $50\ mV\ s^{-1}$ in a solution of 1 M $HClO_4$ with and without 1 M CH_3OH, potential ranging from −0.2 to 1.0 V. CO stripping experiments were performed as follows: after purging the solution with N_2 gas for 20 min, gaseous CO was bubbled for 20 min to allow adsorption of CO onto the electro-catalysts while maintaining a constant voltage of 0.1 V versus SCE. Excess CO dissolved in solution was purged out with N_2 for 20 min and CO stripping voltammetry was recorded in 1 M $HClO_4$ solution at a scan rate of $20\ mV\ s^{-1}$. The electrochemical measurements were conducted under 25 °C.

3. Results and discussion

As CeO_2 is not good electron conductor, we wish to adsorb Pt nanoparticles on CNTs other than CeO_2 surfaces. Such a concept of catalyst preparation can be illustrated in Fig. 1.

By designing the structure of composite catalyst as shown in Fig. 1, we expect that the Pt nanoparticles are adsorbed on PDDA-coated areas and some Pt nanoparticles may have contacts with CeO_2. In the first step of structural designing of Pt-CeO_2/CNTs, we used PDDA, a water soluble quaternary ammonium polyelectrolyte, to achieve site-selective attachment of Pt nanoparticles. Because PDDA carries cationic charges that can induce electronic adsorption with negatively charged surface, it is commonly used in electrostatic assembling nanoparticles on CNT surface [13], fabricating multilayer films [14] or so. To characterize the surface properties changes after PDDA adsorption on CNTs, zeta potential measurement has been applied during the surface treatment process [15]. As a direct method reflecting surface electrostatic properties in solution, zeta potentials of the samples in our process were measured, as shown in Fig. 2.

During zeta potential measurements, the samples were suspended in deionized water in very low concentrations to make sure that the pH of each system remains unchanged. Therefore, the changes of zeta potential corresponding to different samples can only be ascribed to the material introduced to the surface. From Fig. 2, we can see that the zeta potential of O-CNTs changed to positive values after adsorbing PDDA. This confirmed that the PDDA molecules were indeed adsorbed on

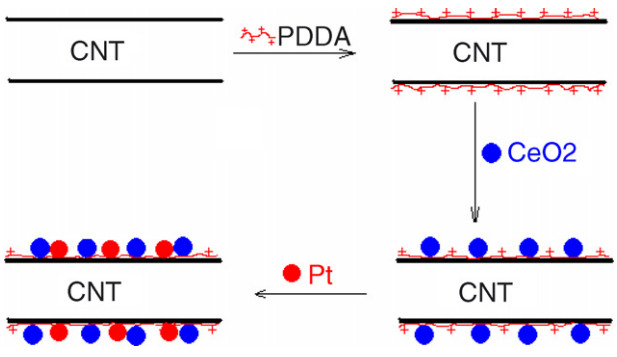

Fig. 1. Schematic diagram of structural designing of Pt-CeO_2/CNTs.

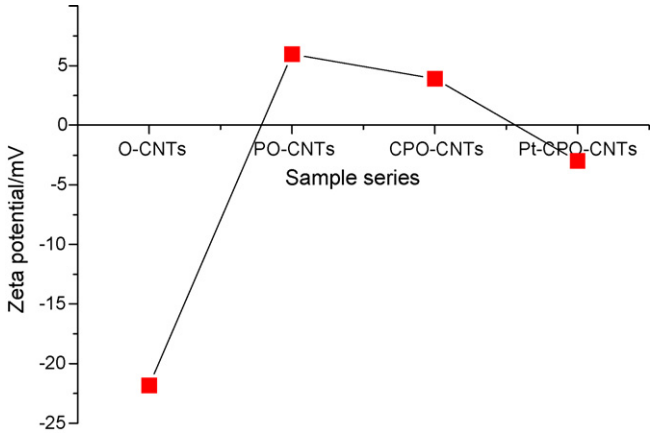

Fig. 2. Zeta potentials of the samples in the catalyst preparation.

the CNTs surface and the cationic charges can therefore be used for adsorbing Pt nanoparticles in the third step, as illustrated in Fig. 1. After depositing CeO_2 on PO-CNTs, the zeta potential of CPO-CNTs only changed a little compared with that of PO-CNTs and was still positive. The positive charges on CPO-CNTs can then act as sites for adsorbing Pt nanoparticles. After adsorbing Pt nanoparticles the zeta potential shifted to negative value. Such results indicate that the Pt nanoparticles are negatively charged. So it is reasonable to assume that Pt nanoparticles are adsorbed on the PDDA-coated areas, where there are positive charges.

To obtain information on the chemical composition of the prepared samples, EDX analysis was conducted and the elemental composition is listed in Table 1.

From Table 1, we can see that the Pt contents in both samples are in agreement with the theoretical content of 20% and the CeO_2 content also approaches the theoretical content of 30%.

Table 1
EDX analysis of the elemental composition of Pt-O-CNTs and Pt-CPO-CNTs

	C (wt.%)	O (wt.%)	Ce (wt.%)	Pt (wt.%)
Pt-O-CNTs	74.02	3.71	–	22.27
Pt-CPO-CNTs	53.43	7.16	20.54	18.87

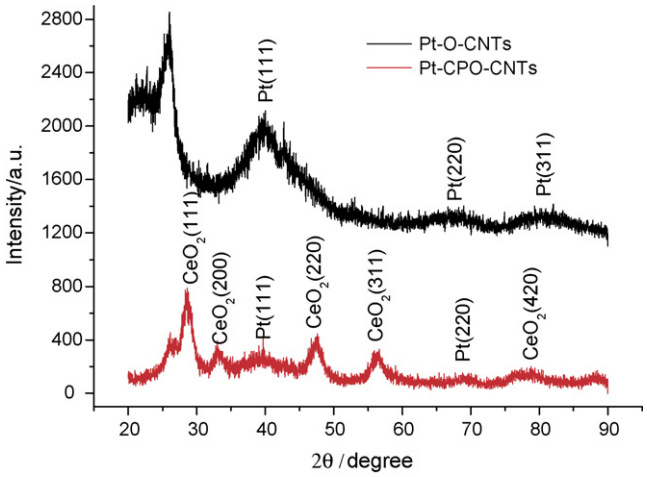

Fig. 3. XRD patterns for Pt-O-CNTs and Pt-CPO-CNTs.

Fig. 3 compares XRD patterns for Pt-O-CNTs and Pt-CPO-CNTs. Both samples show peaks characteristic of Pt, that is, (1 1 1) at $2\theta = 39.8$, (2 2 0) at $2\theta = 68.3$, and (3 1 1) at $2\theta = 80.9$. In the XRD pattern for Pt-CPO-CNTs, five diffraction peaks [(1 1 1), (2 0 0), (2 2 0), (3 1 1), and (4 2 0)] of CeO_2 were observed, corresponding to $2\theta = 28.5$, 33, 47.5, 56.3, and 79, respectively. From the XRD patterns we can see that Pt and CeO_2 coexist in Pt-CPO-CNTs.

The TEM images of CPO-CNTs and Pt-CPO-CNTs were shown in Fig. 4(a and b), respectively. As can be seen in Fig. 4(a),

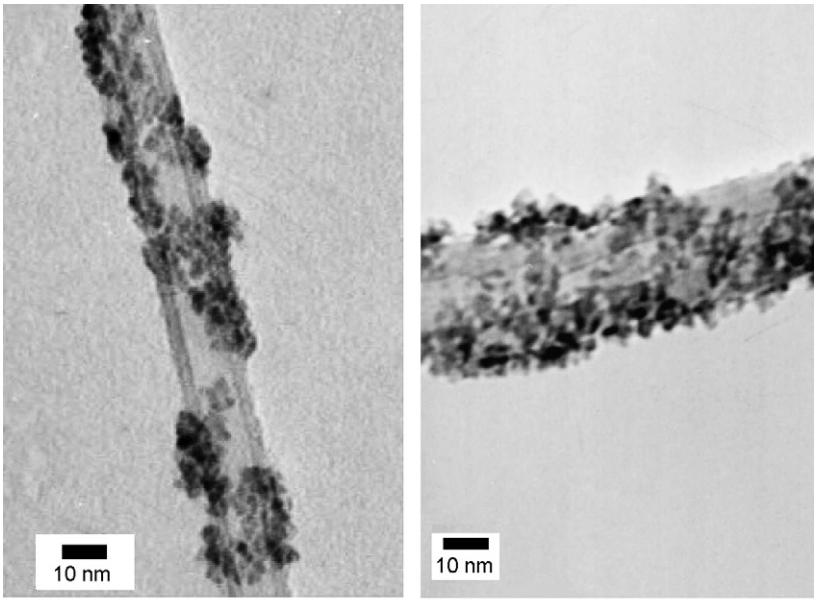

(a) (b)

Fig. 4. TEM images of CPO-CNTs and Pt-CPO-CNTs: (a) CPO-CNTs and (b) Pt-CPO-CNTs.

there is non-uniform coatings of CeO_2 nanoparticles over PO-CNTs, so the uncoated areas can be left for Pt adsorption. For the Pt-CPO-CNTs shown in Fig. 4(b), it is difficult to distinguish Pt nanoparticles from CeO_2 nanoparticles, so we analyzed the structure of the Pt-CPO-CNTs catalyst using HRTEM, as shown in Fig. 5.

From Fig. 5, we can see that there are at least two cases for Pt nanoparticles location on CNT surface. One case is that some Pt nanoparticles have contacts with CeO_2, as can be seen from the adjacent nanoparticles with different lattice spacing, ~0.2233 and ~0.3143 nm, corresponding to Pt [1 1 1] and CeO_2 [1 1 0] [16], respectively. Another case is that some Pt nanoparticles are deposited on CNT surface with no contact with CeO_2, as can be seen from the nanoparticle with lattice spacing of ~0.2197, which can be attributed to Pt [1 1 1].

To see the size distribution of the prepared Pt nanoparticles, we accounted randomly 100 Pt nanoparticles on O-CNTs, as shown in Fig. 6(a). It can be seen that the Pt nanoparticles are homogeneously distributed over O-CNTs and the average size is about 2.5 nm.

As for the influences of CeO_2 on Pt catalysis for methanol electro-oxidation, we compared the Pt-O-CNTs and Pt-CPO-CNTs in terms of electrochemical active surface (EAS) areas and methanol electro-oxidation activity using CV methods. EAS is calculated by assuming that Pt surface is covered by monolayer adsorbed H and taking 0.21 mC cm^{-2} as the reference [17] and the Pt utilization can be reflected in terms of EAS per unit weight Pt. The results are shown in Figs. 7 and 8, respectively.

From Figs. 7 and 8, we can see that the EAS areas of Pt-O-CNTs and Pt-CPO-CNTs have no large differences while the methanol electro-oxidizing current is significantly increased as for the latter catalyst. The data were analyzed and listed in Table 2.

From the EAS_m values listed in Table 2, that is, 520 cm^2 mg^{-1} Pt for Pt-O-CNTs and 515 cm^2 mg^{-1} Pt for Pt-CPO-CNTs, we can see that the EAS_m of the Pt-CPO-CNT did not change very much, which supported indirectly that the Pt nanoparticles are selectively deposited and the side-effects of bad electron conductivity of CeO_2 is avoided. On the other hand, the methanol

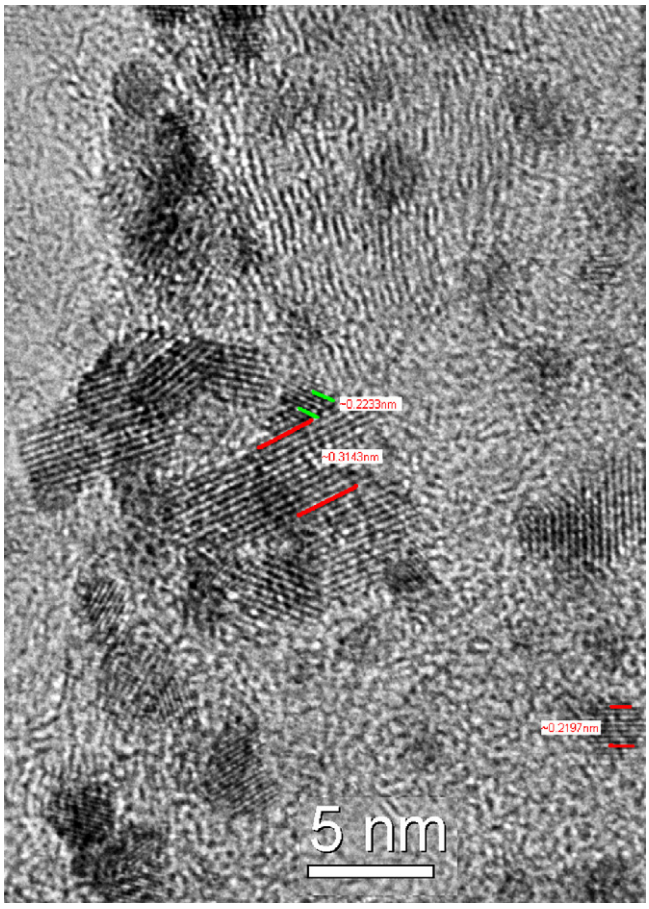

Fig. 5. HRTEM images of Pt-CPO-CNTs.

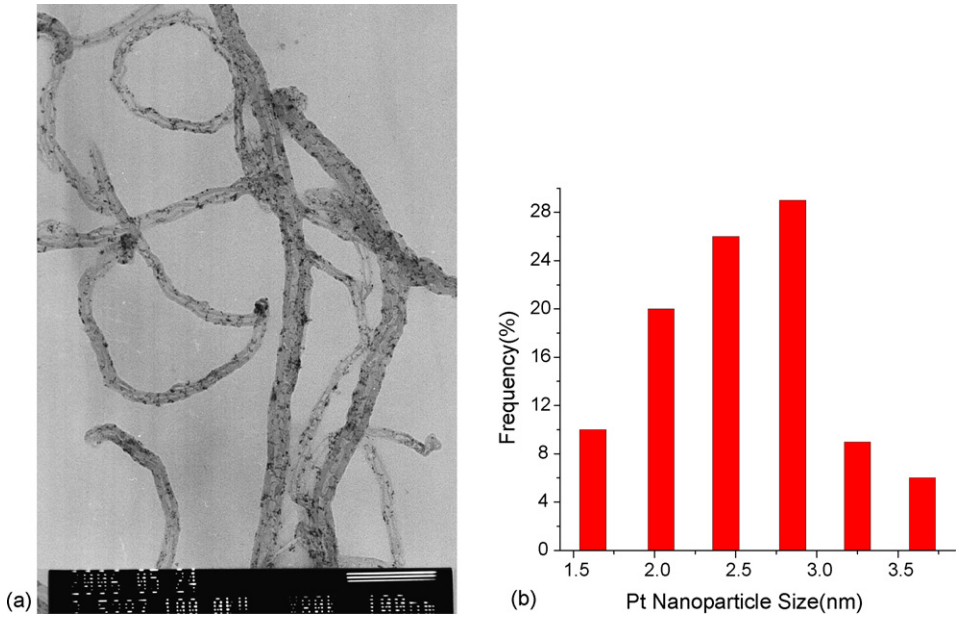

Fig. 6. (a) TEM image for Pt-O-CNTs and (b) particles size distribution for Pt-O-CNTs.

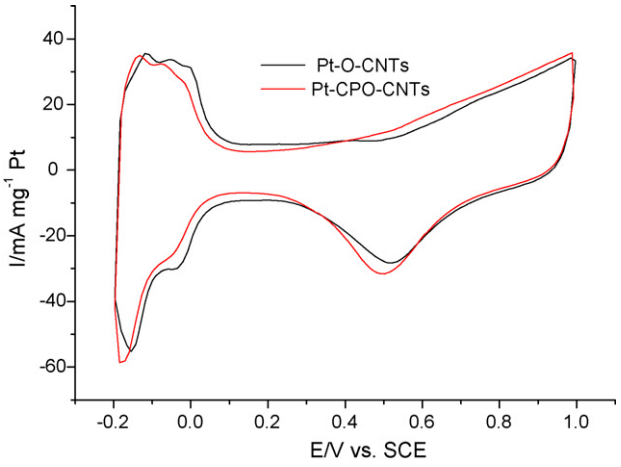

Fig. 7. Voltammetry curves for Pt-O-CNTs and Pt-CPO-CNTs in 1 M $HClO_4$.

Table 2
Data collected fromFigs. 7 and 8

	EAS_m[a] ($cm^2\ mg^{-1}$ Pt)	E_{onset} (V)	I_m[a] ($mA\ mg^{-1}$ Pt)
Pt-O-CNTs	520	0.543	383
Pt-CPO-CNTs	515	0.505	638

[a] The subscript 'm' denotes that the EAS and current are mass normalized.

electro-oxidizing current (I_m) is increased from 383 to 638 A g^{-1} after introducing CeO_2 into the catalyst, as can be seen in Table 2. The results show that by designing the structure of catalyst, we can promote the catalyzing effect of Pt with no apparent decrease of EAS. On the other hand, the onset potential (E_{onset}) of Pt-CPO-CNTs is lower than that of Pt-O-CNTs. This fact indicates that methanol is more easily electro-oxidized on Pt-CPO-CNTs than on Pt-O-CNTs.

To compare the potentiostatic behavior of the two catalysts, we recorded the chronoamperometry curves for Pt-O-CNTs and Pt-CPO-CNTs in 1 M $HClO_4$ and 1 M CH_3OH at 0.6 V for 3000 s, as shown in Fig. 9. From Fig. 9, it can be seen that the current for Pt-CPO-CNTs keeps higher than that for Pt-O-CNTs during the whole test range, indicating that the former is more active than the latter for methanol electro-oxidation, as is consistent with the CV results.

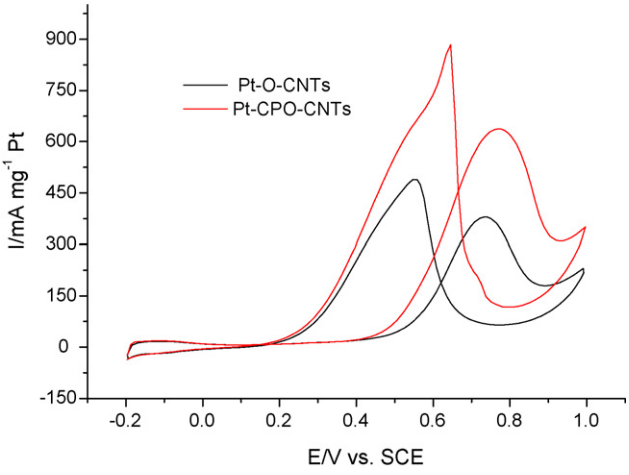

Fig. 8. Voltammetry curves for Pt-O-CNTs and Pt-CPO-CNTs in 1 M $HClO_4$ +1 M CH_3OH.

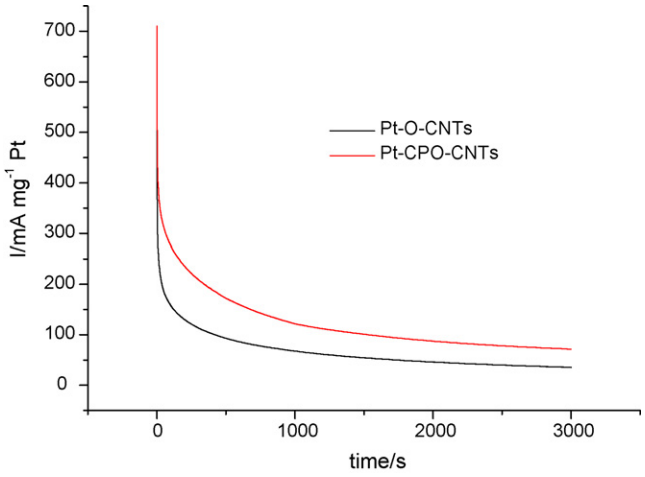

Fig. 9. Chronoamperometry curves for Pt-O-CNTs and Pt-CPO-CNTs in 1 M $HClO_4$ + 1 M CH_3OH at 0.6 V.

Since CO species are the main poisoning intermediate, a good catalyst for methanol electro-oxidation should possess excellent CO electro-oxidizing ability, which can be reflected from CO stripping test. To analyze the mechanism behind the enhanced electro-catalyzing activity of Pt for methanol electro-oxidation (as shown in Fig. 8), we compared the two catalysts in terms of CO eliminating ability, as shown in Fig. 10. From Fig. 10, it can be seen that the CO stripping potential of the Pt-CPO-CNTs shifts to a lower value compared with that of Pt-O-CNTs. Such a result indicates that CeO_2 can

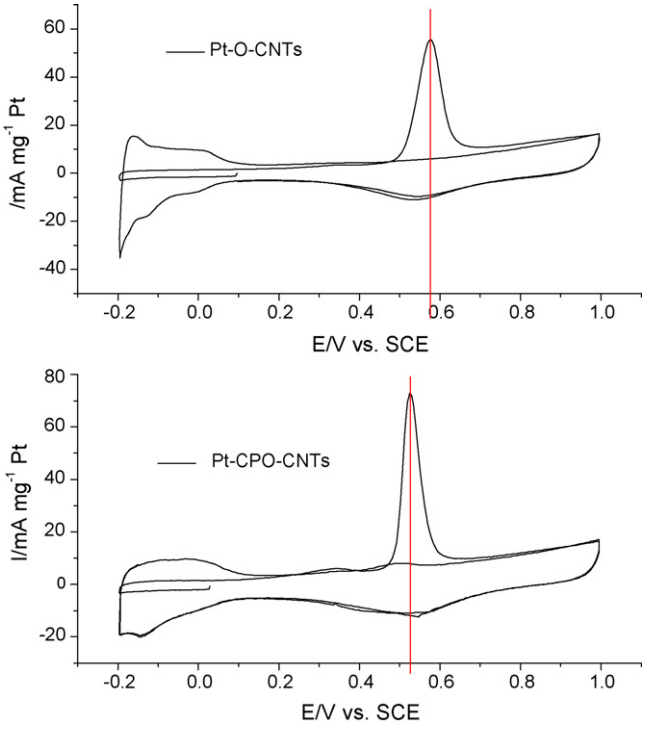

Fig. 10. CO stripping curves for Pt-O-CNTs and Pt-CPO-CNTs.

make CO oxidation easier under lower potential, which may be one reason for increased methanol electro-oxidizing current in Fig. 8.

As the CO electro-oxidation can be promoted by CeO_2, the mechanism of CO electro-oxidation can be tentatively deduced as:

$$CeO_2 + H_2O \rightarrow CeO_2\text{-}OH_{ads} + H^+ + e$$

$$Pt\text{-}CO_{ads} + CeO_2\text{-}OH_{ads} \rightarrow Pt + CeO_2 + CO_2 + H^+ + e$$

It can be taken for granted that only when Pt nanoparticles have contacts with CeO_2 can the CO electro-oxidation be promoted. As shown in Fig. 5, there are some Pt particles that have no contact with CeO_2. Even so, the methanol electro-oxidation current were still greatly promoted with CeO_2 addition. If the Pt loading on CNTs is increased, the contact area between Pt and CeO_2 will increase accordingly, and the methanol electro-oxidation activity will increase more significantly. The work towards this direction will be done in details later.

4. Conclusion

In this study, Pt-CeO_2/CNTs were prepared by adsorbing Pt nanoparticles on CeO_2 coated CNTs. Zeta potential analysis, HRTEM and voltammetry (CV) methods indicated that Pt nanoparticles were selectively adsorbed on CNTs other than CeO_2 surface. Compared with Pt supported on CNTs, Pt-CeO_2/CNTs exhibited higher catalytic activity for methanol electro-oxidation, and the corresponding CO stripping potential shifted to a lower value, indicating that CeO_2 can make CO electro-oxidation easier, which is helpful for CO and methanol electro-oxidation.

Acknowledgements

The authors appreciate the financial support of the State Key Basic Research Program of PRC (2002CB211803) and National Natural Science Foundation of China (90410002).

References

[1] T. Yajima, H. Uchida, M. Watanabe, J. Phys. Chem. B 108 (2004) 2654–2659.
[2] J.M. Léger, S. Rousseau, C. Coutanceau, F. Hahn, C. Lamy, Electrochim. Acta 50 (2005) 5118–5125.
[3] C. Lu, C. Rice, R.I. Masel, P.K. Babu, P. Waszczuk, H.S. Kim, E. Oldfield, A. Wieckowski, J. Phys. Chem. B 106 (2002) 9581–9589.
[4] F. Colmati, E. Antolini, E.R. Gonzalez, Electrochim. Acta 50 (2005) 5496–5503.
[5] L.H. Jiang, G.Q. Sun, Z.H. Zhou, S.G. Sun, Q. Wang, S.Y. Yan, H.Q. Li, J. Tian, J.S. Guo, B. Zhou, Q. Xin, J. Phys. Chem. B 109 (2005) 8774–8778.
[6] K.W. Park, J.H. Choi, B.K. Kwon, S.A. Lee, H.Y. Ha, S.A. Hong, Y.E. Sung, H. Kim, A. Wieckowski, J. Phys. Chem. B 106 (2002) 1869–1877.
[7] S. Mukerjee, R.C. Urian, S.J. Lee, E.A. Ticianelli, J. McBreen, J. Electrochem. Soc. 151 (2004) A1094–A1103.
[8] K.W. Park, K.S. Ahn, Y.C. Nah, J.H. Choi, Y.E. Sung, J. Phys. Chem. B 107 (2003) 4352–4355.
[9] S. Carrettin, P. Concepcion, A. Corma, J.M.L. Nieto, V.F. Puntes, Angew. Chem. Int. Ed. 43 (2004) 2538–2540.
[10] C.W. Xu, P.K. Shen, J. Power Sources 142 (2005) 27–29.
[11] H.B. Yu, J.H. Kim, H.I. Lee, M.A. Scibioh, J. Lee, J. Han, S.P. Yoon, H.Y. Ha, J. Power Sources 140 (2005) 59–65.
[12] Z.L. Liu, J.Y. Lee, W.X. Chen, Langmuir 20 (2004) 181–187.
[13] M.A. Correa-Duarte, N. Sobal, L.M. Liz-Marzan, M. Giersig, Adv. Mater. 16 (2004) 23–24.
[14] R.Z. Ma, T. Sasaki, Y. Bando, J. Am. Chem. Soc. 126 (2004) 10382–10388.
[15] B. Kim, W.M. Sigmund, Langmuir 20 (2004) 8239–8242.
[16] C.C. Tang, Y.S. Bando, B.D. Liu, D. Golberg, Adv. Mater. 17 (2005) 3005–3009.
[17] R.Z. Yang, X.P. Qiu, H.R. Zhang, J.Q. Li, W.T. Zhu, Z.X. Wang, X.J. Huang, L.Q. Chen, Carbon 43 (2005) 11–16.